

1 **Potential impact of land use change on future regional climate in the Southeastern U.S.:**
2 **Reforestation and crop land conversion.**

3 M. Trail¹, A.P. Tsimpidi¹, P. Liu¹, K. Tsigaridis^{2,3}, Y. Hu¹, A. Nenes^{4,5}, B. Stone⁶, and A.G
4 Russell¹

5
6 ¹School of Civil & Environmental Engineering, Georgia Institute of Technology, Atlanta, GA
7 30332, USA

8 ²Columbia Univ, Ctr Climate Syst Res, New York, NY USA

9 ³NASA, Goddard Inst Space Studies, New York, NY 10025 USA

10 ⁴ School of Earth & Atmospheric Sciences, Georgia Institute of Technology, Atlanta, GA
11 30332, USA

12 ⁵School of Chemical and Biomolecular Engineering, Georgia Inst. Technology, Atlanta, GA
13 30332, USA

14 ⁶School of City and Regional Planning, Georgia Inst. Technology, Atlanta, GA 30332, USA

15
16

17 **Abstract**

18 The impact of future land use and land cover changes (LULCC) on regional and global
19 climate is one of the most challenging aspects of understanding anthropogenic climate change.
20 We study the impacts of LULCC on regional climate in the southeastern U.S. by
21 downscaling the NASA Goddard Institute for Space Studies (GISS) global climate model E to
22 the regional scale using a spectral nudging technique with the Weather Research and
23 Forecasting (WRF) Model. Climate-relevant meteorological fields are compared for two
24 southeastern U.S. LULCC scenarios to the current land use/cover for four seasons of the year
25 2050. In this work it is shown that reforestation of cropland in the southeastern U.S. tends to
26 warm surface air by up to 0.5 K while replacing forested land with cropland tends to cool the
27 surface air by 0.5 K. Processes leading to this response are investigated and sensitivity
28 analyses conducted. The sensitivity analysis shows that results are most sensitive to changes
29 in albedo and the stomatal resistance. Evaporative cooling of croplands also plays an
30 important role in regional climate. Implications of LULCC on air quality are discussed.
31 Summertime warming associated with reforestation of croplands could increase the
32 production of some secondary pollutants while a higher boundary layer will decrease pollutant
33 concentrations; wintertime warming may decrease emissions from biomass burning from
34 wood stoves.

35

36 **1 Introduction**

37 Humans have changed the global environment for centuries and our impact has
38 intensified over recent decades due to increased population and intensification of industrial
39 activity. A considerable forcing for global change is land use and land cover changes
40 (LULCC). The impact of future LULCC on atmospheric temperatures and global climate is
41 of growing interest as it can impact human and ecosystem health. Increased importance has
42 been given to the study of LULCC impact on climate at a regional level rather than studying
43 the changes in the global mean radiative forcing because “it is the regional responses, not a
44 global average, that produce drought, floods, and other societally important climate impacts”
45 [Mahmood *et al.*, 2010]. The National Research Council (NRC) recently reported that
46 “Improving societally relevant projections of regional climate impacts will require a better
47 understanding of the magnitudes of regional forcings and the associated climate responses”
48 [NRC, 2005]. The NRC includes LULCC as an area that has an impact on climate which is
49 highly variable by region.

50 Beginning in the 1700s and continuing through the 19th century, the southeastern U.S.
51 underwent intense land use and land cover changes [Chen *et al.*, 2006; Pacala *et al.*, 2001;
52 Prestemon and Abt, 2002; Steyaert and Knox, 2008; Wear and Greis, 2002]. The South
53 experienced forest clearing from the 1700s up to the 1930s, a trend which has been reversed in
54 the past few decades with the growth of the timber industry [Wear and Greis, 2002]. Even
55 though there has been significant reforestation since 1930, the 214 million acres of currently
56 forested land in the South only constitutes 60 % of the forested land that existed in 1630
57 [Wear and Greis, 2002]. The Southeast now produces 60% of the nation’s timber products
58 [Prestemon and Abt, 2002] and in the past 30 years, pine plantations have rapidly increased
59 (from 2 million acres in 1953 to more than 30 million acres in 1999) [Conner and Hartsell,
60 2002.]. These trends are slated to continue given the growing demand to develop forest-to-
61 fuel technologies, as well as to increase wood products-related industries. While changes in
62 mobile source fuels may lead to improvements in global climate (or decreases in the projected
63 warming trend) [Bull, 1996; Leiby and Rubin, 2003], the implications of LULCC with regard
64 to climate change are less understood [Akhtar *et al.*, 2008; IPCC, 2007; Jihee *et al.*, 2008;
65 Skamarock *et al.*, 2005; Stooksbury, 2008].

66 Climate impacts of global- and regional-scale LULCC have been studied using both
67 observations and models [Beltran-Przekurat *et al.*, 2012; Cai and Kalnay, 2004; Chase *et al.*,
68 2000; Christy *et al.*, 2006; Davin and de Noblet-Ducoudre, 2010; Fall *et al.*, 2010b; Kalnay

69 *and Cai, 2003; Lawrence and Chase, 2010; Nunez et al., 2008; Pielke et al., 2011*]. Global
70 LULCC studies have shown that afforestation at high latitudes typically tends to warm the
71 atmosphere while afforestation at equatorial latitudes tends to cool. The effects of
72 afforestation at mid-latitudes however are highly uncertain. Bala et al. [2007] used the
73 Lawrence Livermore National Laboratory INCCA (Integrated Climate and Carbon) model
74 [*Bala et al., 2005; Thompson et al., 2004*] to simulate the interactions within the climate
75 system including those from LULCC. They found that while the decrease in carbon uptake
76 due to global deforestation would have a warming effect, the biophysical (albedo) changes
77 would induce cooling that would overwhelm the warming associated with carbon in most
78 areas of the globe, particularly in Northern high latitudes. Fall et al.[2010] used observation
79 minus reanalysis (OMR) methods to estimate the impacts of historical land cover changes on
80 temperature trends in North America. Fall et al. determined in their study that historical
81 warming trends can be explained on the basis of LULCC and that climate models should
82 include LULCC along with the typical greenhouse-gas driven radiative forcings. Arora and
83 Montenegro [2011] also simulate future global warming in their study to investigate the
84 impacts of potential realistic LULCC scenarios, rather than extreme cases such as complete
85 deforestation, on climate, where they conclude that any global cooling associated with
86 realistic afforestation is not large enough to take the place of global greenhouse-gas emissions
87 reductions.

88 More recent global LULCC studies have analyzed the impacts of biophysical changes
89 that impact radiative processes (albedo) as well as those that impact nonradiative processes,
90 such as partitioning of sensible and latent heat transfer [*Davin and de Noblet-Ducoudre, 2010;*
91 *Lawrence and Chase, 2010*]. Davin et al. [2010] used the Institut Pierre-Simon (IPSL)
92 climate model [*Marti, 2005*] to investigate the climate impacts of individual biophysical
93 parameters associated with LULCC. The study reveals the significance of changes in
94 evaporation and surface roughness as well as albedo on climate. Similarly, Lawrence et al.
95 [2010] use the Community Climate System Model [*Lawrence and Chase, 2007*] to show that,
96 in some afforested regions, nonradiative processes like evapotranspiration can have a cooling
97 effect that overwhelms warming associated with decreased albedo. Beltran-Przekurat et al.
98 [2012] also focused on analyzing the effects of changes in heat flux partitioning, surface
99 roughness and albedo on temperature but concentrated over a region in South America. They
100 found that changes in regional climate are correlated with changes in diurnal heat flux
101 partitioning.

102 In this paper, we use the spectral nudging technique for dynamic downscaling of
103 global model results to the regional scale and compare resulting climate relevant
104 meteorological fields of two southeastern U.S. LULCC scenarios and a base case scenario for
105 four seasons of the year 2050. The downscaling technique used is a type 4 as discussed by
106 [Castro *et al.*, 2005]. In our previous work [Liu *et al.*, 2012] we examined the performance of
107 two nudging techniques, grid and spectral nudging, by downscaling NCEP/NCAR data using
108 the Weather Research and Forecasting (WRF) Model and showed that spectral nudging can
109 outperform grid nudging at the small scale while preserving the large scale features. We also
110 compare future versus present day downscaled meteorological fields in previous work [Trail,
111 2013] using spectral nudging to downscale the NASA Goddard Institute for Space Studies
112 (GISS) global climate model E results during the years 2006 to 2010 and 2048 to 2052 over
113 the continental United States and predicted an average warming of 1-3 °C during the summer
114 and fall in the southeastern U.S. In this study, we use the same approach to simulate
115 meteorological fields for the year 2050 for current day LULCC, a reforested Southeast
116 scenario, and an increased cropland scenario. The role of specific processes and parameters
117 are investigated. We also discuss some of the implications of LULCC on regional air quality.
118 The downscaling technique and choice of physics parameterizations used were evaluated in
119 Trail *et al* [2013] by comparing them with in situ observations for the present year.

120

121 **2 Model Approach**

122

123 2.1 Global Model

124 Lateral boundary and initial conditions for the regional forecast modeling are taken
125 from the GISS ModelE2 [Schmidt, 2013]. The model has a horizontal resolution of 2°×2.5°
126 latitude by longitude. The model has 40 layers which follow a sigma coordinate up to 150 hPa,
127 with constant pressure layers between 150 and 0.1 hPa. Simulations are carried out for the
128 calendar years 2006-2010 and 2048-2052 with a 3 year spinup time for each period, driven by
129 possible future atmospheric conditions over the 21st century and follow the scenario
130 development process for IPCC AR5. This study uses the “Representative Concentration
131 Pathway” (RCP) 4.5 scenario [Lamarque *et al.*, 2011; Moss *et al.*, 2010] where global
132 emissions of greenhouse gases, short-lived species, and land-use-land-cover produce an
133 anthropogenic radiative forcing at 4.5 W m⁻² (approximately 650 ppm CO₂-equivalent) in the
134 year 2100 [2010]. Physical and chemical parameters were produced at 6-hour intervals for

135 regional downscaling by WRF (section 2.2). Further details of the global simulations can be
136 found in Trail et al. [2013].

137

138 2.2 Regional Model

139

140 The Weather Research and Forecasting (WRF) Model [Skamarock and Klemp, 2008]
141 version 3.4 is used as the regional simulation model. The modeling domain includes the
142 contiguous United States (CONUS) and southern Canada and northern Mexico. The domain
143 is centered at 40°N and 97°W with dimensions of 164×138 horizontal grids cells (5940×5004
144 km) with 36-km horizontal grid-spacing and the top level at 50hPa (~15.9 km above ground)
145 (Figure 1). Planetary boundary layer dynamics are simulated using the Yonsei University
146 (YSU) [Hong et al., 2006] scheme; the Noah scheme [Ek et al., 2003] is used for land surface
147 model (LSM). The long-wave Rapid Radiative Transfer Model (RRTM) [Mlawer et al.,
148 1997] and Dudhia scheme [Dudhia, 1989] are used for longwave and shortwave radiation
149 respectively. A revised version of the Kain-Fritsch scheme [Kain J. S., 1993] is used to
150 represent the effects of both deep and shallow cumulus clouds while cloud microphysics are
151 simulated based on Lin et al. [Lin et al., 1983].

152 Key parameters used by WRF associated with LULCC that impact climate include
153 albedo, stomatal resistance (RS), leaf area index (LAI), and surface roughness (Z^0) [Pielke et
154 al., 1998]. Albedo is the fraction of solar energy reflected. Stomatal resistance refers to the
155 leaf's resistance to release moisture into the atmosphere, affecting whether energy is released
156 as sensible or latent heat. Leaf area index is defined as the one-sided green leaf area per unit
157 ground surface area ($LAI = \text{leaf area} / \text{ground area}, \text{m}^2 / \text{m}^2$). The LAI and stomatal resistance
158 are used by the Noah scheme to calculate transpiration via the Jarvis mechanism which also
159 takes into account water availability, photosynthetically active radiation (PAR), and CO₂
160 concentration. Surface roughness is a parameter used to calculate the turbulent diffusion of
161 energy and represents the height of the land cover, and affects whether energy is transferred to
162 the atmosphere as sensible or latent heat. Here, the MM5 Monin-Obukhov surface layer
163 scheme in WRF uses the surface roughness to calculate latent and sensible heat flux via
164 standard similarity functions.

165 In the USGS 24-category landuse dataset, the standard data currently used for WRF
166 simulations, the Southeast is primarily made up of evergreen needleleaf forest, dryland
167 cropland and pasture, deciduous broadleaf forest, and mixtures of these. Two southeastern
168 LULCC scenarios and a base scenario were simulated in this study (Figure 2): one in which

169 all types of current cropland are replaced by evergreen needleleaf (“SE_for”), and one in
170 which all types of forest or forest mixture are replaced by dryland cropland and pasture
171 (“SE_crop”). Evergreen needleleaf forest is chosen due to its commercial use. Evergreen
172 needleleaf forest in the USGS dataset is a combination of the various species of evergreen
173 needleleaf trees and does not differentiate loblolly and slash pine from other species, which
174 may have different physiological characteristics. Loblolly and slash pine make up the
175 majority of the species of pine in the Southeast. Dryland cropland and pasture in the USGS
176 dataset includes semi-irrigated crops, or crops that are irrigated with overhead sprinklers,
177 which make up most of the cropland in the Southeast. There is an irrigated cropland category
178 but this refers to heavily irrigated crops such as rice paddies and is not prevalent in the
179 Southeast where crops are made up of cotton, wheat, corn and others. The base case
180 simulation will be referred to as SE_norm.

181 In addition, sensitivity analyses are conducted to determine which model land use
182 parameters have the greatest influence on regional climate, and how changes in those
183 parameters affect results. We calculated the sensitivity of regional meteorological variables to
184 individual parameters including surface roughness height (Z^0), albedo, leaf area index (LAI),
185 emissivity, and stomatal resistance (RS). Wintertime (DJF) and summertime (JJA)
186 sensitivities to a parameter are calculated by changing the dryland/cropland parameter of
187 interest to that of evergreen needleleaf land cover, and separately to that of deciduous
188 broadleaf forest. Sensitivity simulations are conducted for three-month periods. Table 1
189 contains details of the vegetative parameters and Table 2 contains the sensitivity test
190 parameters. The resulting seasonal mean meteorology is then compared to the base case
191 meteorology over regions where dryland/cropland is the dominant land use.

192 We do not include simulated changes in atmospheric composition-induced radiative
193 forcing due to LULCC, such as the change in greenhouse gases due to carbon uptake of crops
194 and forests, or the changes in the direct and indirect aerosol effect associated with changes in
195 biogenic emissions and air quality.

196 197 2.3 Dynamical downscale of global results

198
199 Spectral nudging is used with a wave number of 2 in both zonal and meridional
200 directions to account for the large scale GCM simulation, but allow the small scale features
201 expected from LULCC in the southeastern U.S. to freely develop [Liu *et al.*, 2012]. In other
202 words, no nudging is conducted at wavelengths shorter than the preset value. A wavelength

203 of 2 corresponds to about 1500 km, which is larger than the spatial scale of changes simulated
204 here. Spectral nudging is applied to temperature, horizontal winds, and geopotential height.
205 No nudging is conducted for variables within the planetary boundary layer (PBL), with the
206 exception of the horizontal winds which are nudged at all vertical levels. The nudging
207 coefficient for all nudged variables was set to $3 \times 10^{-4} \text{ s}^{-1}$ [Stauffer and Seaman, 1990].
208 Nudging is conducted every 6 h during the simulation, consistent with the frequency of the
209 global model data.

210 Trail et al. [2013] found that the model predictions agree well with observations when
211 conducted for 2010. They show that the simulated temperature agrees best with surface
212 observations over the southern U.S., particularly during summer. Simulated wind speed had a
213 root mean square error (RMSE) as low as 2.2 m s^{-1} over the South. While details of the base
214 simulation are given in Trail et al. [2013], they are briefly summarized here in Tables A1 and
215 A2.

216

217 **3 Results**

218 3.1 Southeast reforestation scenario (“SE_for”)

219 3.1.1 Land cover change and affected parameters

220

221 The two major LULCC occurring in the Southeast reforestation scenario are the
222 conversion of dryland/cropland and pasture to evergreen needleleaf forest (which will be
223 referred to as “crop” and “pine”, respectively) and conversion of cropland/woodland mosaic
224 (or “crop/wood”) to pine (Figure 2). It is important to note that crop/wood has parameters
225 that represent a combination of not only crop and pine, but also of deciduous broadleaf forest.
226 There is also a small region in south Georgia where cropland/grassland mosaic is converted to
227 pine, however this region is small compared to the other two LULCC. A large region of crop
228 is converted to pine in southern Louisiana and continuing north along the western borders of
229 Mississippi and Tennessee. Crop is also converted to pine in Florida and in a large region
230 beginning in south Georgia and continuing in a streaking pattern across the eastern regions of
231 South and North Carolina. Crop/wood is converted to pine in the northern regions of the land
232 cover change area including Missouri, Tennessee, and North Carolina, as well as regions in
233 western Mississippi and some in the middle of Florida.

234 In this simulation the albedo of pine is 0.12 all year, meaning that, within that land use
235 category, 12% of the incoming solar radiation is reflected away from the Earth’s surface
236 (Table 2). The albedo of crop, on the other hand, is higher than pine and changes from 0.17 to

237 0.23 depending on the time of year, with the lowest albedo occurring when crops are green
238 and the higher when cropland appears whiter and there is increased soil exposure after harvest.
239 Impacts of snow cover on albedo are simulated as well. Correspondingly, in regions where
240 crop is converted to pine, the albedo change causes 10-12% less reflected solar radiation
241 during the winter and fall and only 5-10% less during the spring and summer (Figure A1a).
242 The albedo of crop/wood varies from 0.16 to 0.2 depending on the time of year and the
243 corresponding decreased albedo and seasonal change is reflected in Figure A1a over regions
244 where crop/wood is converted to pine.

245 The LAI is correlated to albedo since a higher leaf area index usually means more
246 green area to absorb sunlight. However, the combined effect of LAI and stomatal resistance
247 plays another important role in climate because it drives sensible and latent heat flux
248 partitioning via transpiration. Heat flux partitioning, in turn, strongly impacts temperature
249 and planetary boundary layer (PBL) dynamics [Pielke *et al.*, 1998]. In WRF, the RS is
250 calculated using the Jarvis mechanism where a minimum RS is adjusted by various forcings
251 (ie, sunlight, temperature, relative humidity, and soil moisture availability). RS for crop and
252 pine are 40 and 125 s m⁻¹ respectively. In other words, pine trees are more resistant to
253 releasing water and latent heat than crops. During the winter, the LAI increases by up to 4
254 units (leaf area per area) in regions where the land cover is converted to pine (Figure A1b).
255 Similar to the change in albedo, the difference in LAI decreases during the spring and more so
256 during the summer as crops grow and produce more leaves. During summer, in regions where
257 crop changes to pine, the difference in LAI is only slightly positive (less than 1 unit area area⁻¹
258 ¹), while the LAI difference is higher (up to 2.5 units area area⁻¹) in regions where crop/wood
259 changes to pine. We see a greater difference in LAI over regions where crop/wood changes to
260 pine during the summer because, as mentioned earlier, crop/wood includes some parameters
261 from deciduous broadleaf forest which has a lower LAI than that of pine.

262 Changing surface roughness impacts turbulence within the boundary layer which
263 affects the transfer of momentum, heat and water vapor from the Earth's surface. Increasing
264 Z^0 causes more energy to be transferred as latent heat and less as sensible heat. However, the
265 direct implications with regard to climate change are not very well known [Davin and de
266 Noblet-Ducoudre, 2010]. The Z^0 of pine and crop/wood remain constant throughout the year
267 at 0.5 m and 0.2 m, respectively while the Z^0 of crop (between 0.05 and 0.15 m) is smaller
268 during the winter (Table 1). Again, as crops grow during the spring and summer, the
269 difference in Z^0 decreases slightly in regions where crop is converted to pine.

270

271 3.1.2 Impacts on meteorology

272 A heating pattern of up to 0.5 degrees occurs during the winter over most of the areas
273 where crop and crop/wood are converted to pine (Figure 3a). P-values resulting from a paired
274 t-test show significant temperature anomalies over regions that are converted to pine (Figure
275 A2). The average diurnal changes in temperature over regions where crop is converted to
276 pine show that this heating occurs during the day, while at night the temperature does not
277 change nearly so much (Figure A3 and A4). The decreased albedo attributed to converting
278 from inactive and exposed soil crop to green pine during the winter drives the heating in these
279 regions (Figure A1a). However, since Z^0 increases with pine reforestation, the winter heating
280 is diminished slightly, although not overcome, by the increase in latent heat flux via
281 evapotranspiration. Also, the daytime boundary layer height increases by 10% on average
282 where crop is converted to pine because more of the energy flux is realized as sensible heat
283 (Figure A3) [Pielke *et al.*, 1998]. During the spring we see a similar heating of around 0.3
284 degrees mostly over regions where crop is converted to pine. We did not find significant
285 changes in precipitation due to the LULCC perturbations.

286 Interesting patterns of cooling in Louisiana near the Mississippi river (up to 0.5
287 degrees decrease) and warming in South Carolina and southern Georgia (up to 0.5 degrees
288 increase) over regions where crop is converted to pine occur during the summer and continue
289 through the fall (Figure 3a). Changes in precipitation may explain some cooling during the
290 summer when Louisiana receives approximately 2 mm more rain per day in the afforested
291 scenario while net rain near the eastern coast changes little. However, during the fall there is
292 little apparent change in precipitation over the two regions (Figure A5). Despite little
293 differences in precipitation, there is still an increase in soil moisture in Louisiana during both
294 summer and fall (Figure 3b). Pine has a higher RS and over time, water is allowed to
295 accumulate throughout the season in the soil near the Mississippi river rather than be
296 evaporated. Correspondingly, the diurnal latent heat flux in Louisiana increases during the
297 daytime in the summer, cooling the surface air, while in Georgia and the Carolinas the
298 increase in latent heat flux is not as strong, leading to an increase in sensible heat flux to
299 maintain the energy balance, causing the warming (Figure 4). Recent studies show that
300 temperature changes alone do not completely characterize changes in surface air heat content
301 because some energy is stored in moisture in the air, and suggest using an equivalent
302 temperature which takes into account the latent heat energy [Fall *et al.*, 2010a]. While
303 cooling occurs during the summer and fall over the Mississippi river, the change in equivalent

304 temperature (Figure 3c) shows an increase in surface heat air content equivalent of up to a
305 degree.

306

307 3.2 Southeast cropification scenario (“SE_crop”)

308 3.2.1 Land cover change and affected parameters

309

310 There are four major LULCC that occur in the Southeast cropification scenario where
311 the following four land covers are converted to dryland/cropland and pasture (or “crop”):
312 evergreen needleleaf forest (or “pine” as before), cropland/woodland mosaic (“crop/wood” as
313 before), deciduous broadleaf forest (“deciduous”), and mixed forest (Figure 2). The region
314 where pine is converted to crop, the largest LULCC in this scenario, covers almost all of
315 Louisiana, Mississippi, Alabama, Georgia, and South Carolina except where crop already
316 existed. The pine to crop conversion also extends to southern Arkansas and northern Florida.
317 In this scenario, crop/wood is converted to crop in the same regions where crop/wood is
318 converted to pine in the Southeast reforestation scenario discussed earlier. Deciduous forest is
319 converted to crop in large regions of northern Arkansas and southern Missouri, as well as
320 some parts of Tennessee. Some mixed forest is converted to crop in eastern Tennessee and
321 parts of North Carolina.

322 In this scenario the albedo increases for all LULCC and all seasons except for regions
323 where mixed forest is converted to crop (Figure A6a). The most dramatic increase of albedo
324 is in the large regions where pine is converted, due to the year round low albedo of pine.
325 Spring and summer see a less intense increase (around 5%) in albedo when the crops emerge.
326 Also during the spring and summer, the albedo of crop/wood, deciduous, and mixed forest are
327 all nearly the same as that of crop (0.16 to 0.17 from Table 2).

328 The LAI decreases with the conversion of pine to crop mostly during the winter (up to
329 3.5 units area area⁻¹), less during the spring and fall (around 2 units area area⁻¹), and only
330 slightly during the summer (less than 1 unit area area⁻¹) (Figure A6b). The LAI also decreases
331 slightly for all other LULCC during the winter. However, during the summer the LAI
332 increases for all other LULCC with the highest increase over regions where deciduous is
333 converted to crop (more than 2 units area area⁻¹). In this scenario, RS decreases from between
334 70 and 125 s m⁻¹ to 40 s m⁻¹. The surface roughness decreases for all LULCC and for all
335 seasons with the biggest decreases happening during the winter where pine and deciduous
336 change to crop.

337

338 3.2.2 Impacts on meteorology

339

340 Most regions in the Southeast are cooled with future cropification (Figure 5a) with the
341 largest and most significant (Figure A2; p-values < 0.05) decreases occurring during the
342 summer over northern Mississippi and Alabama and southern Tennessee (over 0.6 degree
343 decrease). Similarly, decreases in surface air heat content are found over most of the region
344 of LULCC (Figure 5c). During the winter, average cooling during the hottest hour of the day
345 reaches 0.5 degree over regions where pine is converted to crop (Figure A7). Increases in
346 albedo over regions where deciduous and pine forests are converted to crop drives the cooling
347 during the winter, despite the warming effect that is expected from the decrease in Z^0 and
348 latent heat flux. Also, boundary layer height during the daytime drops by an average of 100 m
349 (more than 10% decrease) where pine changes to crop (Figure A7), and slightly less where
350 deciduous changes to crop, because boundary layer depth is reduced when less of the energy
351 flux is realized as sensible heat [Pielke et al., 1998].

352 In the spring and summer most of the cooling occurs over regions where deciduous is
353 converted to crop (reaching up to 0.8 degree decrease in some areas) and less cooling is seen
354 over other LULCC regions. Cooling in converted deciduous regions is driven by an increase
355 in the albedo and decreased RS. Diurnal heat flux trends (Figure 6) show a decrease in
356 sensible heat flux and an increase in latent heat flux, due to the combined effect of albedo
357 change and increased evapotranspiration from combined RS and LAI change. In contrast,
358 regions changed from pine experience less cooling because LAI and Z^0 decreases exert a
359 warming force via latent heat flux decreases (Figure 6). There is also less soil moisture
360 available for evaporation due to a decrease in RS in some regions (Figure 5b).

361

362 3.3 Integration of Sensitivity Analysis

363

364 Sensitivity analyses were conducted to test the sensitivity of regional climate to albedo,
365 surface roughness, leaf area index, and stomatal resistance. The sensitivity analyses find that
366 surface temperatures and energy flux distributions are more sensitive to RS during the
367 summer than all other sensitivity scenarios (Figure 7) with average surface temperatures
368 increasing by 0.5 degrees during the daytime. Winter temperature and surface fluxes are not
369 sensitive to RS since evaporation is minimal, as is the related energy flux when crops are not
370 in season. Surface temperature and energy flux over cropland are less sensitive to increasing
371 the cropland LAI as compared to those of pine; however when the cropland LAI is reduced to

372 that of deciduous forest the temperature increases slightly during the summer (Figure A8).
373 During summer and winter, the daytime surface temperature in grids dominated by cropland
374 increases by 0.2 degrees when crop albedo is replaced by that of pine. The sensible and latent
375 heat fluxes also increase (Figures 7 and 8). During summer, temperatures tend to decrease
376 due to an increased surface roughness by 0.1 degree while the latent heat is increased and the
377 sensible heat decreased (Figure 7). Temperature and energy fluxes are less sensitive to Z^0
378 during the winter (Figure 8). Sensitivity analyses were also conducted using North American
379 Regional Reanalysis (NARR) data as initial and boundary conditions. These sensitivity
380 analyses were conducted with and without using spectral nudging and using 2010 NARR data
381 (Figures A9 through A12). In the case that spectral nudging is used (Figures A9 and A10),
382 the sensitivity results are nearly identical to the results using GISS fields as initial and
383 boundary conditions. With no spectral nudging (Figures A11 and A12), we see increased
384 sensitivity of surface temperature to albedo and stomatal resistance, while the sensitivity to
385 surface roughness and leaf area index remain near zero.

386

387 **4 Discussion**

388

389 The simulated impacts of LULCC in the Southeast on regional climate were expected
390 given the changes in land use parameters (eg. albedo, RS, LAI and Z^0). Reforestation of crop
391 regions in the Southeast tends to lead to warming primarily due to the increase of RS and
392 decrease in albedo while the Z^0 increase may lessen the degree of warming by shifting the
393 transfer of energy to the atmosphere from sensible to latent heat. Warming during the spring,
394 summer and fall can enhance the production of O₃ and secondary PM while, on the other hand,
395 the increased boundary layer height can help decrease concentrations. Warming during the
396 winter may influence less use of wood burning stoves and therefore lead to less emission of
397 PM [Alfarra *et al.*, 2007]. This result compares well with other studies on the impacts of
398 reforestation on climate [Beltran-Przekurat *et al.*, 2012; Betts, 2000; Betts *et al.*, 2007].
399 However, over time, reduced transpiration from increased RS can lead to the accumulation of
400 soil moisture in wet areas such that cooling from soil moisture evaporation overcomes the
401 warming from albedo changes, which is the case for the afforested summer and fall in
402 Louisiana near the Mississippi river. Lawrence and Chase [2010] found similar cooling from
403 reforestation.

404 Our results suggest that cooling tends to occur when forest is replaced with crop in the
405 Southeast, though not enough to counter the simulated warming of 1-3 °C from green house

406 gas increases [Trail et al., 2013]. Cooling during the winter is attributed to the high albedo of
407 cropland while during the spring and summer the decrease in RS also contributes to cooling.
408 Also increased LAI helps cool where deciduous forests are replaced. These results agree with
409 other studies simulating the impacts of cropification [Beltran-Przekurat et al., 2012; Davin
410 and de Noblet-Ducoudre, 2010] as well as looking at historical LULCC and temperature data
411 [Fall et al., 2010b]. Cooling during the winter could cause more emissions of PM from wood
412 burning while during the rest of the year the rate of production of O₃ and secondary PM could
413 decrease.

414 While the results of the LULCC study show that reforestation of cropland does not
415 appear to be an effective method for climate mitigation in the Southeast, the sensitivity
416 analysis shows that these results are sensitive to assumed physical parameters. Some recent
417 studies have found a significant degree of cooling from reforestation in the Southeast [Juang
418 et al., 2007; Murphy et al., 2012]. In particular, Murphy et al, suggest that the stomatal
419 conductance of loblolly pine, the major species of pine in the Southeast, should be adjusted
420 from the default value and this would lead to more simulated cooling in the Southeast
421 [Murphy et al., 2012]. We assumed the default value for stomatal resistance from the USGS
422 24-category landuse data for a combined “evergreen needleleaf” category. Thus, further
423 investigation is needed to minimize uncertainty in the stomatal resistance and to consider the
424 physiological differences between actual loblolly pine and the evergreen needleleaf category
425 typically used as well as the physiological differences among the various crops present in the
426 Southeast. Our results suggest that a reduction in the stomatal resistance of pine equivalent to
427 the Murphy simulations would lead to a cooler surface over pine forest. Juang et al, found
428 that in a region of North Carolina, pine forest tend to be cooler than marginal, or abandoned,
429 fields [Juang et al., 2007]. These fields have less leaf area and lower roughness heights than
430 cropland, and are not subject to irrigation, all of which would tend to make marginal fields
431 warmer than cropland, and potentially warmer than pine forest, especially loblolly pine.

432 |
433 **5 Acknowledgments**
434

435 While this work was supported, in part, by grants from the US EPA (EPA-G2008-
436 STAR-J1) and NASA, reference herein to any specific commercial products, process, or
437 service by trade name, trademark, manufacturer, or otherwise, does not necessarily constitute
438 or imply their endorsement or recommendation. NARR data was provided by the
439 NOAA/OAR/ESRL PSD, Boulder, Colorado, USA, from their Web site at

Formatted

440 <http://www.esrl.noaa.gov/psd/>. The views and opinions of authors expressed herein are those
441 of the authors and do not necessarily state or reflect those of the United States Government.
442

443 6. References

- 444
- 445 Akhtar, F., et al. (2008), Beyond the standards: Designer Air Quality in 2050, *Bulletin of the*
446 *American Meteorological Society*, 89(1), 38-38
- 447 Alfarra, M. R., et al. (2007), Identification of the mass spectral signature of organic aerosols
448 from wood burning emissions, *Environmental Science & Technology*, 41(16), 5770-
449 5777, doi:10.1021/es062289b.
- 450 Bala, G., et al. (2005), Multicentury changes to the global climate and carbon cycle: Results
451 from a coupled climate and carbon cycle model, *Journal of Climate*, 18(21), 4531-
452 4544, doi:10.1175/jcli3542.1.
- 453 Bala, G., et al. (2007), Combined climate and carbon-cycle effects of large-scale deforestation,
454 *Proc. Natl. Acad. Sci. U. S. A.*, 104(16), 6550-6555, doi:10.1073/pnas.0608998104.
- 455 Beltran-Przekurat, A., et al. (2012), Modelling the effects of land-use/land-cover changes on
456 the near-surface atmosphere in southern South America, *Int. J. Climatol.*, 32(8), 1206-
457 1225, doi:10.1002/joc.2346.
- 458 Betts, R. A. (2000), Offset of the potential carbon sink from boreal forestation by decreases in
459 surface albedo, *Nature*, 408(6809), 187-190, doi:10.1038/35041545.
- 460 Betts, R. A., et al. (2007), Biogeophysical effects of land use on climate: Model simulations
461 of radiative forcing and large-scale temperature change, *Agric. For. Meteorol.*, 142(2-
462 4), 216-233, doi:10.1016/j.agrformet.2006.08.021.
- 463 Bull, S. R. (1996), Renewable energy transportation technologies, *Renewable Energy*, 9(1-4),
464 1019-1024
- 465 Cai, M., and E. Kalnay (2004), Climate - Impact of land-use change on climate - Reply,
466 *Nature*, 427(6971), 214-214, doi:10.1038/427214a.
- 467 Castro, C. L., et al. (2005), Dynamical downscaling: Assessment of value retained and added
468 using the regional atmospheric modeling system (RAMS), *Journal of Geophysical*
469 *Research-Atmospheres*, 110(D5), 21, doi:D05108 10.1029/2004jd004721.
- 470 Chase, T. N., et al. (2000), Simulated impacts of historical land cover changes on global
471 climate in northern winter, *Climate Dynamics*, 16(2-3), 93-105,
472 doi:10.1007/s003820050007.
- 473 Chen, H., et al. (2006), Effect of land-cover change on terrestrial carbon dynamics in the
474 southern United States, *J. Environ. Qual.*, 35(4), 1533-1547,
475 doi:10.2134/jeq2005.0198.
- 476 Christy, J. R., et al. (2006), Methodology and results of calculating central california surface
477 temperature trends: Evidence of human-induced climate change?, *Journal of Climate*,
478 19(4), 548-563, doi:10.1175/jcli3627.1.
- 479 Conner, R. C., and A. J. Hartsell (2002.), The Southern Forest Resource Assessment: Chapter
480 16, Forest Area and Conditions, Department of Agriculture, Forest Service, Southern
481 Research Station,.
- 482 Davin, E. L., and N. de Noblet-Ducoudre (2010), Climatic Impact of Global-Scale
483 Deforestation: Radiative versus Nonradiative Processes, *Journal of Climate*, 23(1), 97-
484 112, doi:10.1175/2009jcli3102.1.
- 485 Dudhia, J. (1989), Numerical study of convection observed during the winter monsoon
486 experiment using a mesoscale two-dimensional model, *J. Atmos. Sci.*, 46(20), 3077-
487 3107
- 488 Ek, M. B., et al. (2003), Implementation of Noah land surface model advances in the National
489 Centers for Environmental Prediction operational mesoscale Eta model, *Journal of*
490 *Geophysical Research-Atmospheres*, 108(D22), 16, doi:8851 10.1029/2002jd003296.
- 491 Fall, S., et al. (2010a), Temperature and equivalent temperature over the United States (1979-
492 2005), *Int. J. Climatol.*, 30(13), 2045-2054, doi:10.1002/joc.2094.

493 Fall, S., et al. (2010b), Impacts of land use land cover on temperature trends over the
494 continental United States: assessment using the North American Regional Reanalysis,
495 *Int. J. Climatol.*, 30(13), 1980-1993, doi:10.1002/joc.1996.

496 Hong, S. Y., et al. (2006), A new vertical diffusion package with an explicit treatment of
497 entrainment processes, *Mon. Weather Rev.*, 134(9), 2318-2341

498 IPCC (2007), Climate Change 2007 IPCC Fourth Assessment Report: Synthesis Report, 184
499 pp, IPCC, Geneva, Switzerland.

500 Jihee, S., et al. (2008), The Impacts of Urbanization on Emissions and Air Quality:
501 Comparison of Four Visions of Austin, Texas, *Environmental Science & Technology*,
502 42(19), 7294-7300

503 Juang, J. Y., et al. (2007), Separating the effects of albedo from eco-physiological changes on
504 surface temperature along a successional chronosequence in the southeastern United
505 States, *Geophysical Research Letters*, 34(21), 5, doi:L21408 10.1029/2007gl031296.

506 Kain J. S., F. J. M. (1993), Convective parameterization models: The Kain-Fritsch scheme.
507 Cumulus Convection in Numerical Models, *American Meteorological Society*, 46,
508 165-170

509 Kalnay, E., and M. Cai (2003), Impact of urbanization and land-use change on climate,
510 *Nature*, 423(6939), 528-531, doi:10.1038/nature01675.

511 Lamarque, J. F., et al. (2011), Global and regional evolution of short-lived radiatively-active
512 gases and aerosols in the Representative Concentration Pathways, *Clim. Change*,
513 109(1-2), 191-212, doi:10.1007/s10584-011-0155-0.

514 Lawrence, P. J., and T. N. Chase (2007), Representing a new MODIS consistent land surface
515 in the Community Land Model (CLM 3.0), *J. Geophys. Res.-Biogeosci.*, 112(G1), 17,
516 doi:G01023 10.1029/2006jg000168.

517 Lawrence, P. J., and T. N. Chase (2010), Investigating the climate impacts of global land
518 cover change in the community climate system model, *Int. J. Climatol.*, 30(13), 2066-
519 2087, doi:10.1002/joc.2061.

520 Leiby, P. N., and J. Rubin (2003), Transitions in light-duty vehicle transportation -
521 Alternative-fuel and hybrid vehicles and learning, in *Energy, Air Quality, and Fuels*
522 2003, edited, pp. 127-134.

523 Lin, Y. L., et al. (1983), Bulk parameterization of the snow field in a cloud model, *Journal of*
524 *Climate and Applied Meteorology*, 22(6), 1065-1092, doi:10.1175/1520-
525 0450(1983)022<1065:bpotsf>2.0.co;2.

526 Liu, P., et al. (2012), Differences between downscaling with spectral and grid nudging using
527 WRF, *Atmospheric Chemistry and Physics*, 12(8), 3601-3610, doi:10.5194/acp-12-
528 3601-2012.

529 Mahmood, R., et al. (2010), Impacts of land use/land cover change on climate and future
530 research priorities, *Bulletin of the American Meteorological Society*, 91(1), 37-+,
531 doi:10.1175/2009bams2769.1.

532 Marti, O., and Coauthors (2005), The new IPSL climate system model: IPSL-CM4, *Note du*
533 *Pole de Modelisation* 26, 86

534 Mlawer, E. J., et al. (1997), Radiative transfer for inhomogeneous atmospheres: RRTM, a
535 validated correlated-k model for the longwave, *Journal of Geophysical Research-*
536 *Atmospheres*, 102(D14), 16663-16682, doi:10.1029/97jd00237.

537 Moss, R. H., et al. (2010), The next generation of scenarios for climate change research and
538 assessment, *Nature*, 463(7282), 747-756, doi:10.1038/nature08823.

539 Murphy, L. N., et al. (2012), Local and Remote Climate Impacts from Expansion of Woody
540 Biomass for Bioenergy Feedstock in the Southeastern United States, *Journal of*
541 *Climate*, 25(21), 7643-7659, doi:10.1175/jcli-d-11-00535.1.

542 NRC (2005), Radiative Forcing of Climate Change: Expanding the Concept and Addressing
543 Uncertainties, *National Research Council*, 208

544 Nunez, M. N., et al. (2008), Impact of land use and precipitation changes on surface
545 temperature trends in Argentina, *Journal of Geophysical Research-Atmospheres*,
546 113(D6), 11, doi:D06111 10.1029/2007jd008638.

547 Pacala, S. W., et al. (2001), Consistent land- and atmosphere-based US carbon sink estimates,
548 *Science*, 292(5525), 2316-2320, doi:10.1126/science.1057320.

549 Pielke, R. A., et al. (1998), Interactions between the atmosphere and terrestrial ecosystems:
550 influence on weather and climate, *Glob. Change Biol.*, 4(5), 461-475,
551 doi:10.1046/j.1365-2486.1998.t01-1-00176.x.

552 Pielke, R. A., et al. (2011), Land use/land cover changes and climate: modeling analysis and
553 observational evidence, *Wiley Interdiscip. Rev.-Clim. Chang.*, 2(6), 828-850,
554 doi:10.1002/wcc.144.

555 Prestemon, J. P., and R. C. Abt (2002), The Southern timber market to 2040, *Journal of*
556 *Forestry*, 100(7), 16-22

557 Schmidt, G. A., et al (2013), Configuration and assessment of the GISS ModelE2
558 contributions to the CMIP5 archive, *J. Climate*, in preparation

559 Skamarock, W., et al. (2005), A Description of the Advanced Research WRF Version 2.

560 Skamarock, W. C., and J. B. Klemp (2008), A time-split nonhydrostatic atmospheric model
561 for weather research and forecasting applications, *Journal of Computational Physics*,
562 227(7), 3465-3485, doi:10.1016/j.jcp.2007.01.037.

563 Stauffer, D. R., and N. L. Seaman (1990), Use of a 4-dimensional data assimilation in a
564 limited-area mesoscale model .1. Experiments with synoptic-scale data, *Monthly*
565 *Weather Review*, 118(6), 1250-1277, doi:10.1175/1520-
566 0493(1990)118<1250:uofdda>2.0.co;2.

567 Steyaert, L. T., and R. G. Knox (2008), Reconstructed historical land cover and biophysical
568 parameters for studies of land-atmosphere interactions within the eastern United States,
569 *Journal of Geophysical Research-Atmospheres*, 113(D2), 27, doi:D02101
570 10.1029/2006jd008277.

571 Stooksbury, D. (2008), A Primer on Drought History In Georgia, in *Georgia Climate and Air*
572 *Quality Summit*, edited, Atlanta, GA.

573 Thompson, S. L., et al. (2004), Quantifying the effects of CO2-fertilized vegetation on future
574 global climate and carbon dynamics, *Geophysical Research Letters*, 31(23), 4,
575 doi:L23211 10.1029/2004gl021239.

576 Trail, M., Tsimpidi, A. P., Liu, P., Tsigaridis, K., Hu, Y., Nenes, A., and Russell, A. G. (2013),
577 Downscaling a global climate model to simulate climate change impacts on US
578 regional and urban air quality, *Geosci. Model Dev., Discuss.*, 6, 2517-2549,
579 doi:10.5194/gmdd-6-2517-2013.

580 Wear, D. N., and J. G. Greis (2002), Southern Forest Resource Assessment - Summary of
581 findings, *Journal of Forestry*, 100(7), 6-14
582
583
584
585
586
587

Table 1 USGS Land use categories and relevant WRF parameters ^a

Land use Category		RS	LAIMIN (area/area)	LAIMAX (area/area)	ALBEDOMIN	ALBEDOMAX	ZOMIN (m)	ZOMAX (m)
1	'Urban and Built-Up Land'	200	1	1	0.15	0.15	0.5	0.5
2	'Dryland Cropland and Pasture'	40	1.56	5.68	0.17	0.23	0.05	0.15
3	'Irrigated Cropland and Pasture'	40	1.56	5.68	0.2	0.25	0.02	0.1
4	'Mixed Dry/Irr. Cropland and Pasture'	40	1	4.5	0.18	0.23	0.05	0.15
5	'Cropland/Grassland Mosaic'	40	2.29	4.29	0.18	0.23	0.05	0.14
6	'Cropland/Woodland Mosaic'	70	2	4	0.16	0.2	0.2	0.2
7	'Grassland'	40	0.52	2.9	0.19	0.23	0.1	0.12
8	'Shrubland'	300	0.5	3.66	0.25	0.3	0.01	0.05
9	'Mixed Shrubland/Grassland'	170	0.6	2.6	0.22	0.3	0.01	0.06
10	'Savanna'	70	0.5	3.66	0.2	0.2	0.15	0.15
11	'Deciduous Broadleaf Forest'	100	1.85	3.31	0.16	0.17	0.5	0.5
12	'Deciduous Needleleaf Forest'	150	1	5.16	0.14	0.15	0.5	0.5
13	'Evergreen Broadleaf Forest'	150	3.08	6.48	0.12	0.12	0.5	0.5
14	'Evergreen Needleleaf Forest'	125	5	6.4	0.12	0.12	0.5	0.5
15	'Mixed Forest'	125	2.8	5.5	0.17	0.25	0.2	0.5
16	'Water Bodies'	100	0.01	0.01	0.08	0.08	0.0001	0.0001
17	'Herbaceous Wetland'	40	1.5	5.65	0.14	0.14	0.2	0.2
18	'Wooded Wetland'	100	2	5.8	0.14	0.14	0.4	0.4
19	'Barren or Sparsely Vegetated'	999	0.1	0.75	0.38	0.38	0.01	0.01
20	'Herbaceous Tundra'	150	0.41	3.35	0.15	0.2	0.1	0.1
21	'Wooded Tundra'	150	0.41	3.35	0.15	0.2	0.3	0.3
22	'Mixed Tundra'	150	0.41	3.35	0.15	0.2	0.15	0.15
23	'Bare Ground Tundra'	200	0.41	3.35	0.25	0.25	0.05	0.1
24	'Snow or Ice'	999	0.01	0.01	0.55	0.7	0.001	0.001

^aParameters include stomatal resistance (RS), maximum and minimum leaf area index (LAIMAX, LAIMIN), maximum and minimum albedo (ALBEDOMAX, ALBEDOMIN), and maximum and minimum roughness height (ZOMAX, ZOMIN).

591

Table 2 Parameterizations used for each of the sensitivity analyses ^b

Sensitivity Case	'Dryland Cropland and Pasture' parameters						
	RS	LAIMIN (area/area)	LAIMAX (area/area)	ALBEDOMIN	ALBEDOMAX	ZOMIN (m)	ZOMAX (m)
Base	40	1.56	5.68	0.17	0.23	0.05	0.15
ALBp	40	1.56	5.68	0.12	0.12	0.05	0.15
Z ⁰ p	40	1.56	5.68	0.17	0.23	0.5	0.5
RSp	125	1.56	5.68	0.17	0.23	0.05	0.15
LAIp	40	5	6.4	0.17	0.23	0.05	0.15
ALBd	40	1.56	5.68	0.16	0.17	0.05	0.15
Z ⁰ d	40	1.56	5.68	0.17	0.23	0.5	0.5
RSd	100	1.56	5.68	0.17	0.23	0.05	0.15
LAI ^d	40	1.85	3.31	0.17	0.23	0.05	0.15

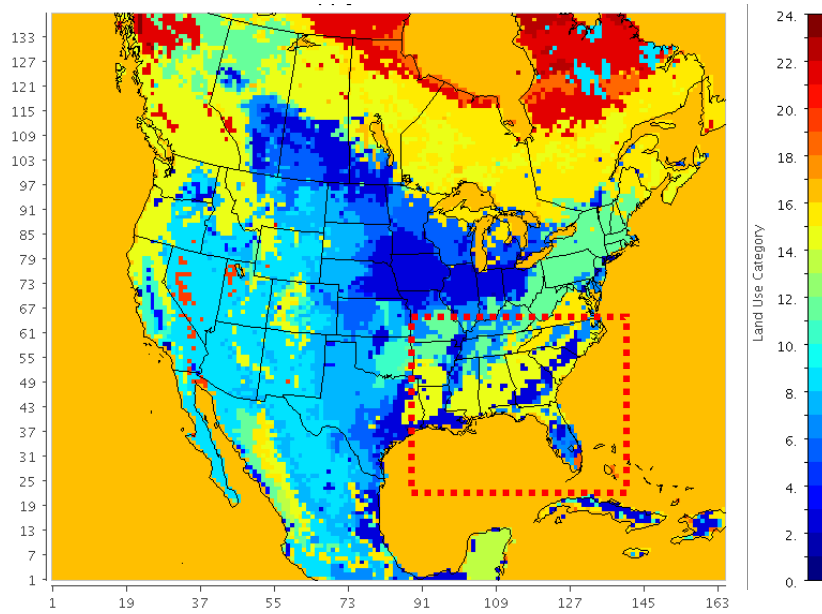
592 ^b Parameters include minimum stomatal resistance (RS), maximum and minimum leaf area index (LAIMAX, LAIMIN), maximum and
593 minimum albedo (ALBEDOMAX, ALBEDOMIN), and maximum and minimum roughness height (ZOMAX, ZOMIN). The name of each
594 sensitivity case begins with the parameter that changed and ends with "p" or "d" indicating whether the new parameter is from the pine (p) or
595 deciduous (d) land use category. The affected parameters in each case are highlighted in bold.

596

597

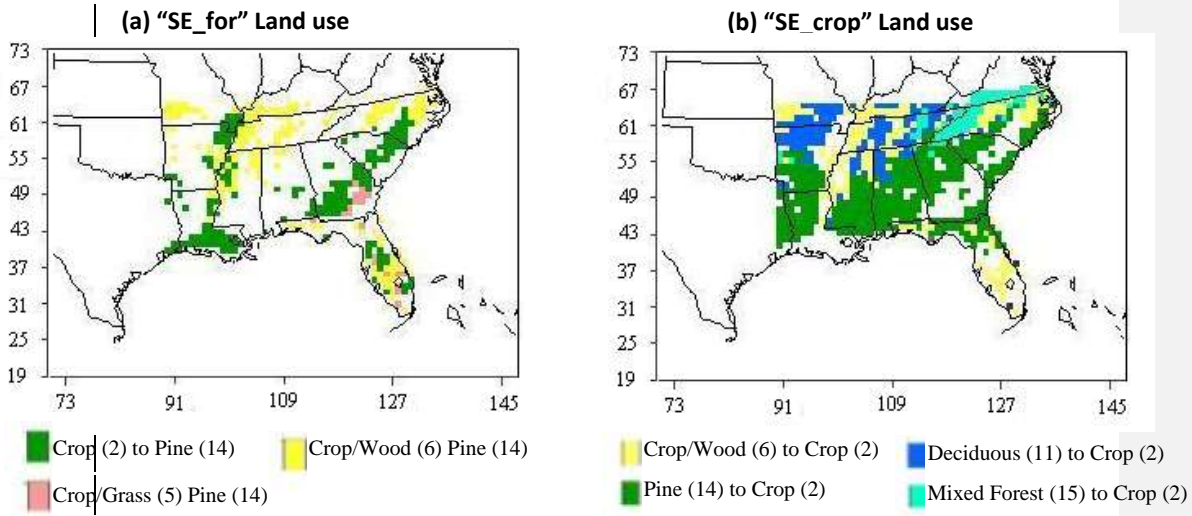
598

599



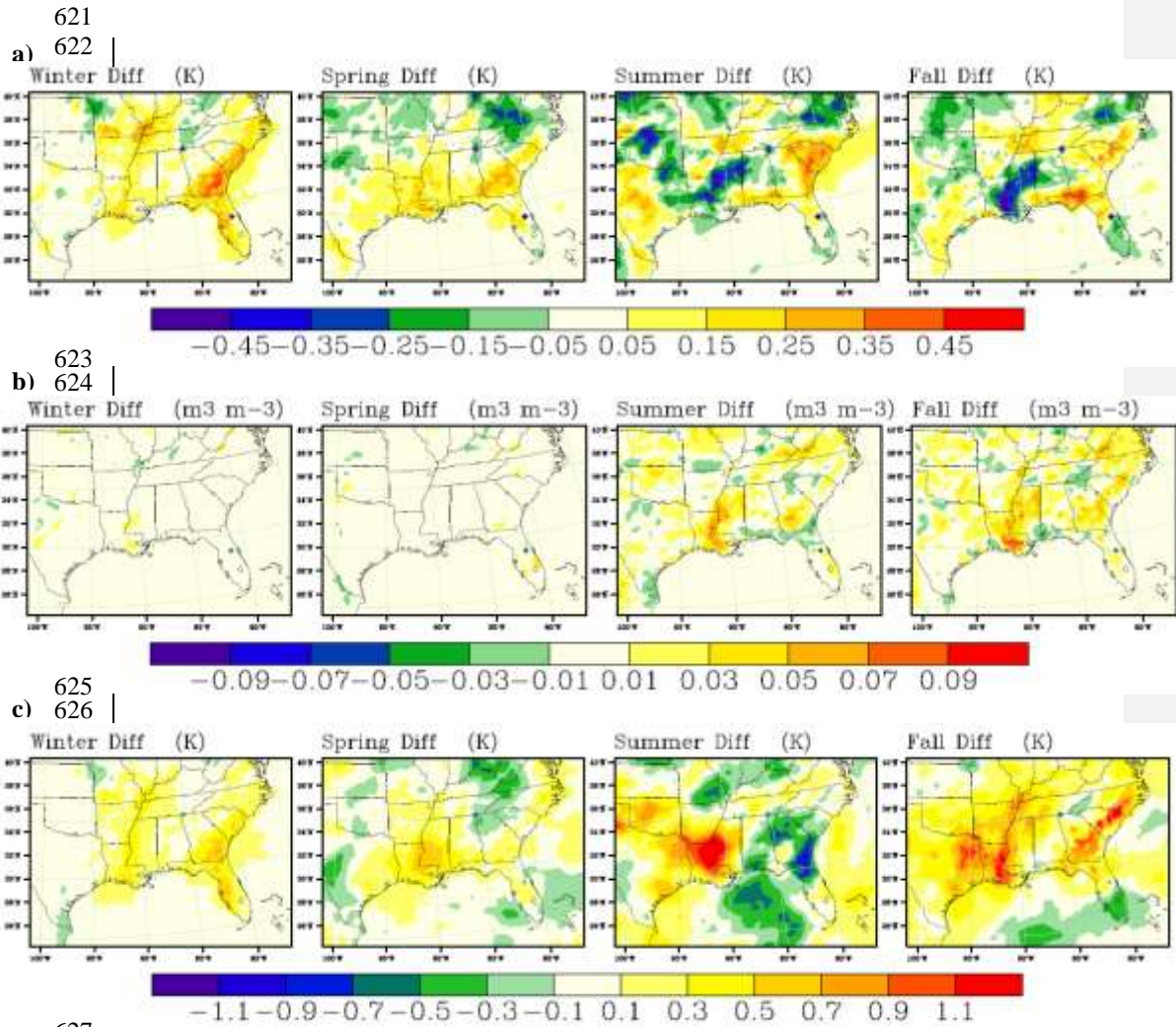
600
 601 **Figure 1** Original dominant land use map of the base case simulation. The area of the tested LULCC scenarios is also shown (red dashed
 602 box). Land use category numbers from legend correspond to categories in Table 1.
 603
 604
 605
 606

607



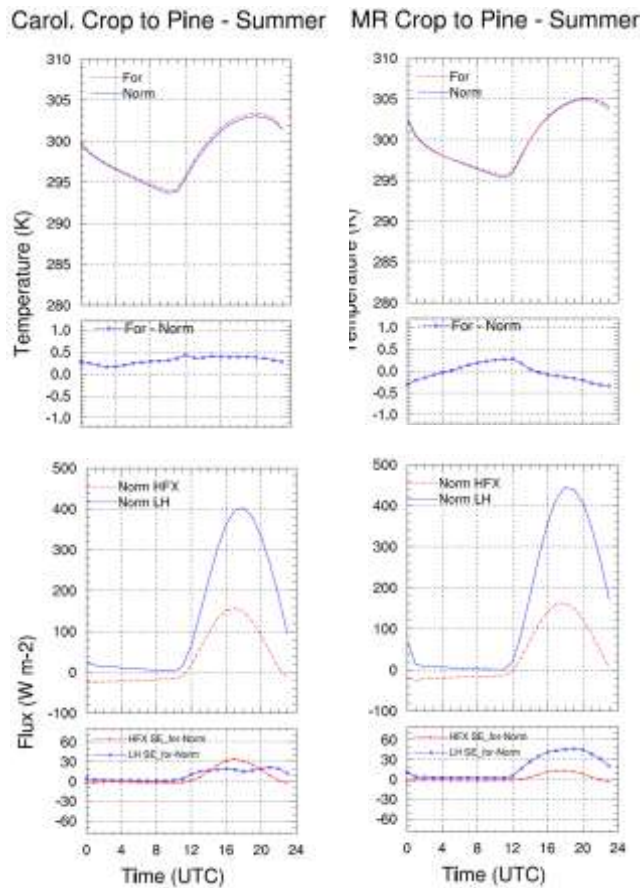
608
609
610
611
612
613
614
615
616
617
618
619
620

Figure 2 Spatial maps of the dominant land use covers that changed to pine (a) and crop (b) in the SE_for and SE_crop scenario respectively. Land use category numbers in parentheses correspond to categories in Table 1



627
628
629 **Figure 3** Simulated temperature (a) soil moisture (b) and equivalent temperature (c) change of SE_for minus SE_norm scenario during the four
630 seasons of the year 2050.
631

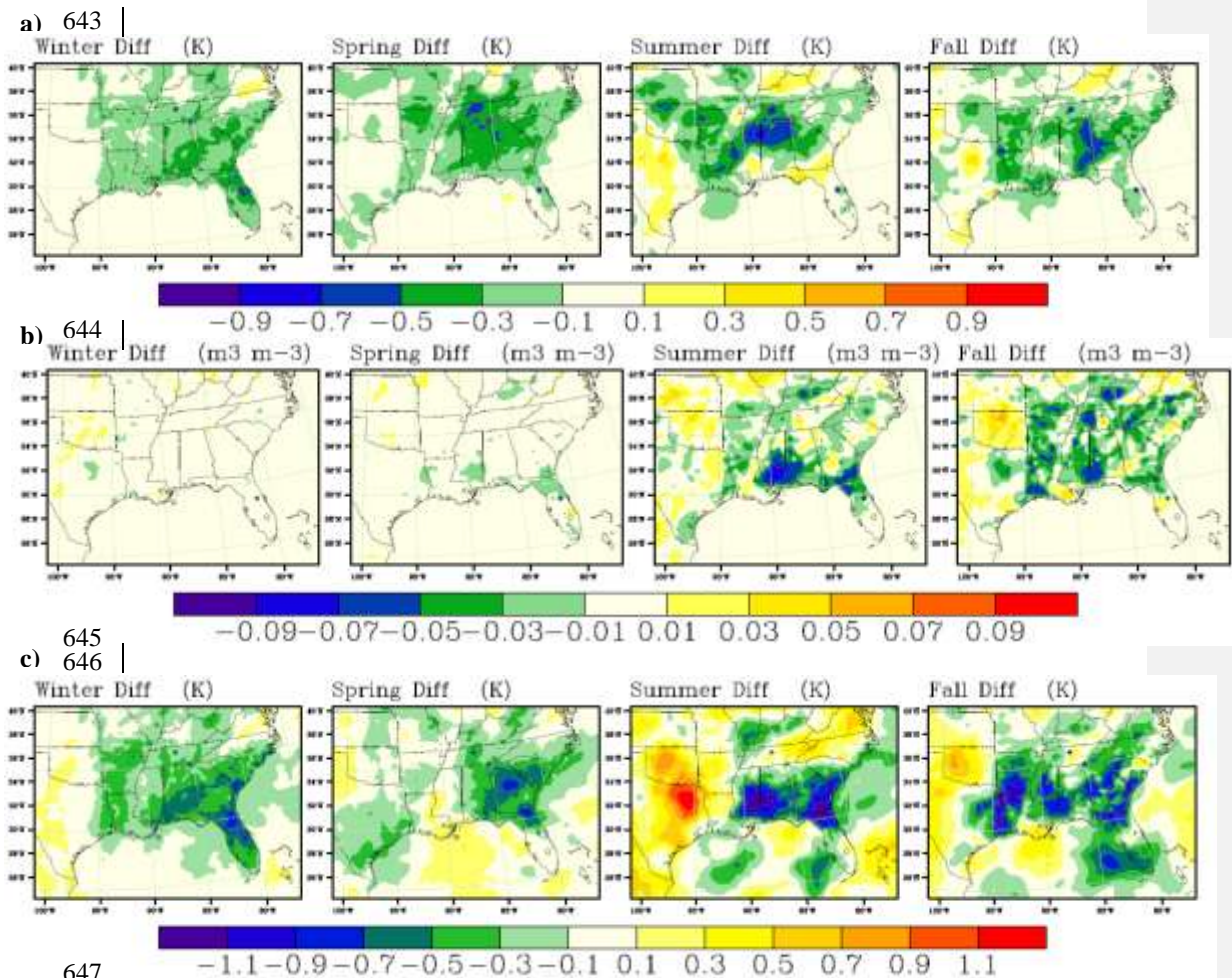
632
633



634

635
636
637
638
639
640
641
642

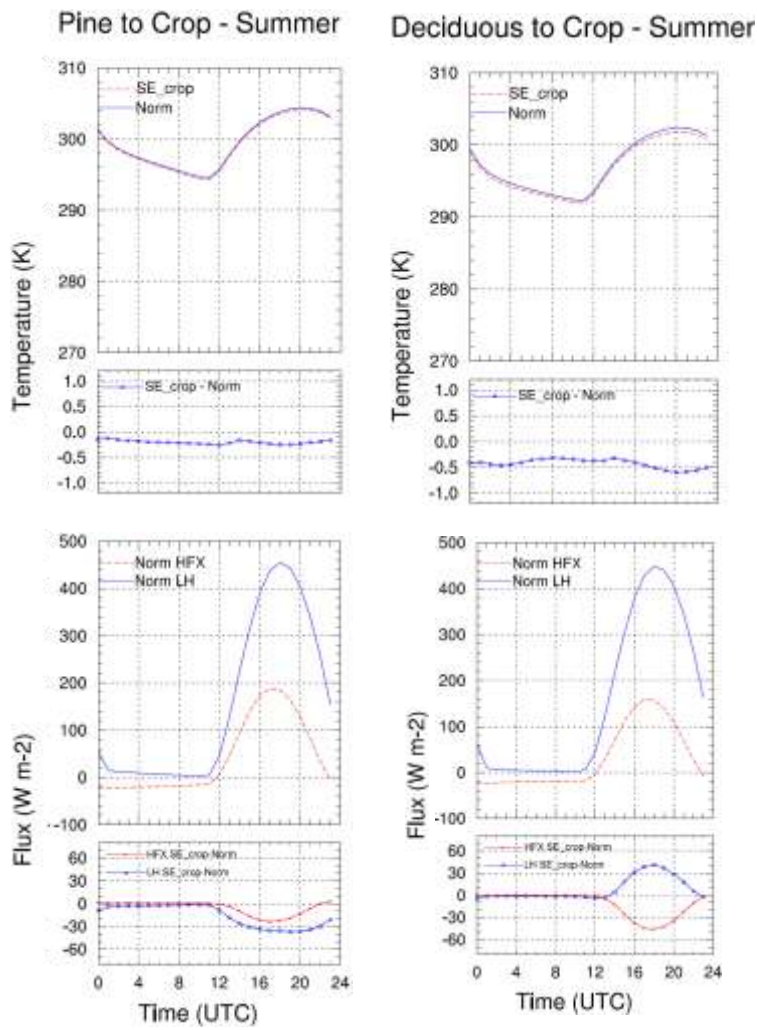
Figure 4 Average diurnal temperature and heat flux trends and anomalies over the grid cells where the dominant land use is converted from crop to pine and separated by the Carolinas and Mississippi river (MR) regions during summer of the year 2050. Top row: average diurnal temperature by region and season for “SE_norm” and “SE_for”. Second row: average diurnal temperature anomaly by region and season (“SE_for” minus “SE_norm”). Third row: average diurnal sensible (red) and latent (blue) heat flux to the atmosphere for the “SE_norm” case. Bottom row: average diurnal sensible (red) and latent (blue) heat flux anomalies (“SE_for” minus “SE_norm”).



647
 648
 649
 650
 651

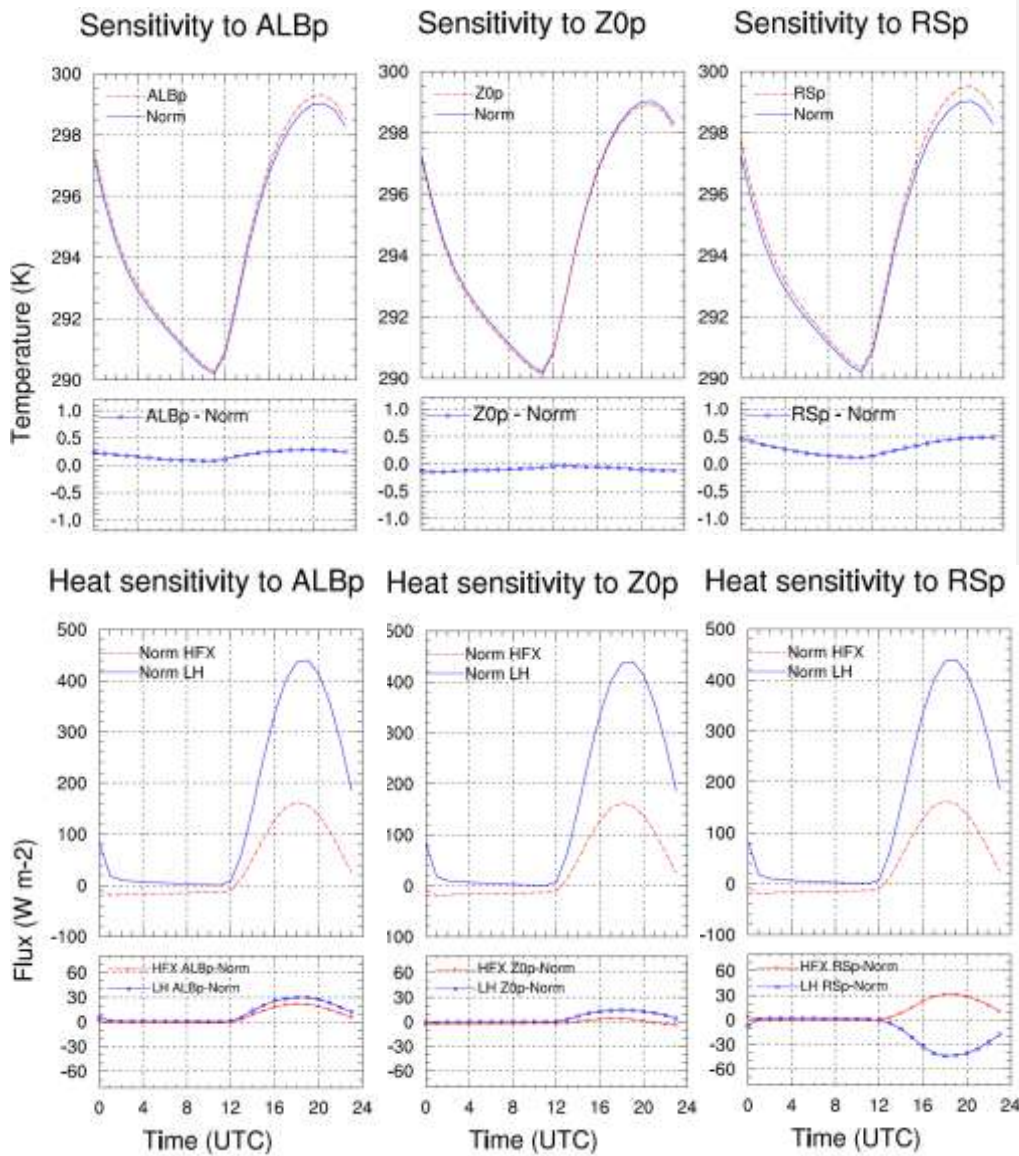
Figure 5 Simulated temperature (a) soil moisture (b) equivalent temperature (c) change of SE_crop minus SE_norm scenario during the four seasons of the year 2050.

652



653
654
655
656
657
658
659
660

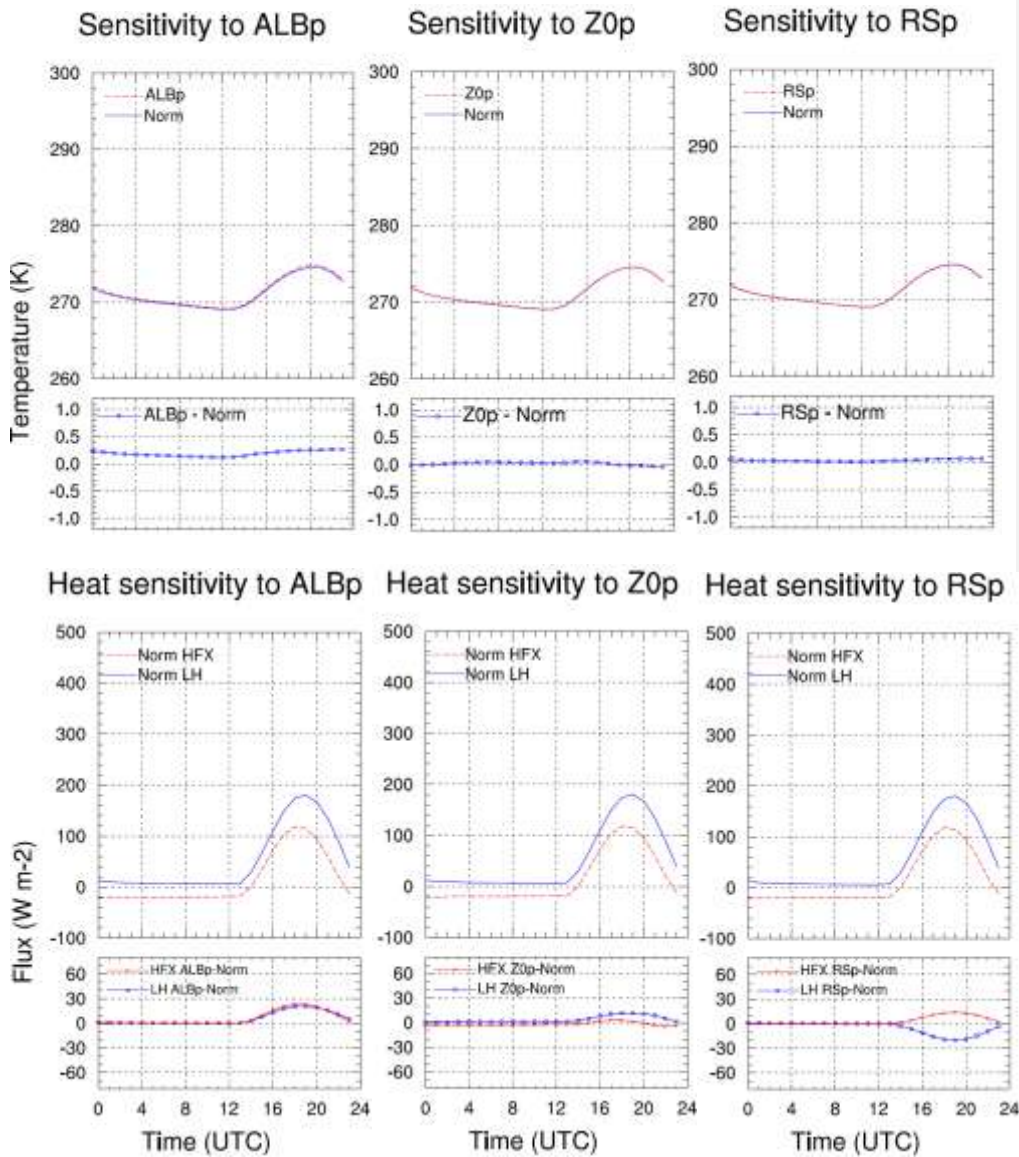
Figure 6 Average diurnal temperature and heat flux trends and anomalies over the grid cells where the dominant land use is converted from pine to crop (left column) and from deciduous to crop (right column) during summer of the year 2050. Top row: average diurnal temperature by season for “SE_norm” and “SE_crop”. Second row: average diurnal temperature anomaly by season (“SE_crop” minus “SE_norm”). Third row: average diurnal sensible (red) and latent (blue) heat flux to the atmosphere for the “SE_norm” case. Bottom row: average diurnal sensible (red) and latent (blue) heat flux anomalies (“SE_crop” minus “SE_norm”).



661
662

663
664
665
666
667
668
669
670

Figure 7 Average diurnal temperature and heat flux trends and sensitivities to pine albedo (ALBp), surface roughness (Z_0^p), and stomatal resistance (RSp) over the grid cells where the dominant land use is crop during summer of the year 2050. Top row: average diurnal surface temperature of the base case (blue) and the perturbed parameter simulation (red). Second row: average diurnal surface temperature sensitivity (perturbed case minus base case). Third row: average diurnal sensible (red) and latent (blue) heat flux to the atmosphere for the base case. Bottom row: average diurnal sensible (red) and latent (blue) heat flux sensitivities (perturbed case minus base case).



671
672

673
674
675
676
677
678
679
680

Figure 8 Average diurnal temperature and heat flux trends and sensitivities to pine albedo (ALBp), surface roughness (Z_0^p), and stomatal resistance (RSp) over grid cells where the dominant land use is crop during winter of the year 2050. Top row: average diurnal surface temperature of the base case (blue) and the perturbed parameter simulation (red). Second row: average diurnal surface temperature sensitivity (perturbed case minus base case). Third row: average diurnal sensible (red) and latent (blue) heat flux to the atmosphere for the base case. Bottom row: average diurnal sensible (red) and latent (blue) heat flux sensitivities (perturbed case minus base case).